ISOTOPE 18O OF ALTERATION ROCKS AT WELL C-1 KAMOJANG GEOTHERMAL FIELD, WEST JAVA, INDONESIA

by Dwi Fitri Yudiantoro

Submission date: 30-Aug-2022 02:17PM (UTC+0700)
Submission ID: 1889295134
File name: 1._1161-2318-1-SM-isotop_O18_Dwi_Fitri-28_Feb_22.pdf (1.37M)
Word count: 10195
Character count: 46705

西南交通大学学报

第 57 卷 第 1 期
2022 年 2 月

JOURNAL OF SOUTHWEST JIAOTONG UNIVERSITY

Vol. 57 No. 1
Feb. 2022

ISSN: 0258-2724

DOI：10.35741/issn.0258-2724.57.1.11

Research article

Earth Sciences

ISOTOPE ^{18}O OF ALTERATION ROCKS AT WELL C-1 KAMOJANG GEOTHERMAL FIELD, WEST JAVA, INDONESIA

印度尼西亚西爪哇岛 C-1 卡莫让 地热场的蚀变岩石同位素 180

D.F. Yudiantoro [a,*], Emmy Suparka [b], Suyanto Yuwono [b], Isao Takashima [c], Daizo Ishiyama [c], Osamu Matsubaya [c], M. Yustin Kamah [d]

[a] Geological Department of UPN "Veteran"
Yogyakarta, Indonesia, d_fitriyudiantoro@upny.ac.id
[b] Geological Department of Institute of Technology
Bandung, Indonesia
[c] Center for Geo-Environmental Science, Akita University,
Akita, Japan
[d] Pertamina Geothermal Energy, Indonesia

Received: December 9, 2021 ▪ Reviewed: January 4, 2022
▪ Accepted: February 2, 2022 ▪ Published: February 28, 2022

Abstract

The purpose of this study is to determine the reservoir condition system of Well C-1. Kamojang geothermal field located in the Quaternary volcanic complex caldera system (0.452 to 1.2 Ma). The volcanic complex contributes to the formation of vapor-dominated high-temperature geothermal systems (250°C). The potential of the electricity produced from this field was 260 MWe. This study describes a new method, namely the ^{18}O isotope of alteration rock, to determine reservoir conditions. Another approach is to use a petrographic analytical form, X-ray diffraction, and isotope ^{18}O and D on some core and cutting samples. Isotope abundances are measured using an isotope ratio mass spectrometer (IRMS). Zoning mineral alteration in Well C-1 comprises the cristobalite-montmorillonite zone, illite-montmorillonite zone, and chlorite-epidote zone. Hydrothermal fluids that generate steam in geothermal systems were derived from meteoric water. These fluids interact with rocks based on the ratio of reservoir water-rock interaction, Well C-1. The research shows that the value of the fraction of oxygen atoms of rocks in the system (1-x) was 0.16. That indicated that the reservoir containing fluid 16% or reservoir is rock-dominated. This research on ^{18}O isotope is a novelty because it differs from what has been done by previous researchers who studied reservoir characteristics using water ^{18}O isotope. Meanwhile, this study uses the ^{18}O isotope of alteration rock to identify reservoir conditions. It is hoped that this method can be used in other geothermal fields.

Keywords: isotope, fluids, reservoir

摘要 本研究的目的是确定 C-1 井的储层条件体系。卡莫让地热田位于第四纪火山复杂破火山口系统（0.452 至 1.2 嘛）。火山复合体有助于形成以蒸汽为主的高温地热系统（250oC）。该领域产生的电力潜力为 260 兆瓦。本研究介绍了一种新的方法，即蚀变岩的 180 同位素来确定储层条件。另一种方法是在一些岩心和切割样品上使用岩相分析形式、X 射线衍射和同位素 180 和 D。使用同位素比质谱仪（信息管理系统）测量同位素丰度。C-1 井区带矿物蚀变包括方英石-蒙脱石带、伊利石-蒙脱石带和绿泥石-绿帘石带。在地热系统中产生蒸汽的热液来自大气水。这些流体根据储层水-岩石相互作用的比率与岩石相互作用，C-1 井。研究表明，系统中岩石的氧原子分数（1-x）为 0.16。这表明含有 16%流体的储层或储层以岩石为主。这项关于 180 同位素的研究是一项新颖的研究，因为它与以前使用水 180 同位素研究储层特征的研究人员所做的不同。同时，本研究利用蚀变岩的 180 同位素来识别储层条件。希望这种方法可以应用于其他地热领域.

关键词: 同位素, 流体, 储层

I. INTRODUCTION

Indonesia has the potential for geothermal energy of 27,000 MW, but there is still little that can be developed, which is around 800 MWe. Of the seven geothermal field locations, five of them are in Java, namely Darajat (145 MW), Dieng (60 MWe), Kamojang (140 MWe), Mount Salak or Awibengkok (330 MWe), and Wayang Windu (110 MWe) [1]-[3]. Also, sixty-six geothermal prospects have been identified on the island [2], [4]. Likewise, geothermal manifestations are scattered around the summit of these Quaternary monogenetic and polygenetic volcanoes [5]-[6]. The Kamojang geothermal field is the first geothermal field with a steam-dominated reservoir developed in Indonesia [1], [7]-[8]. The Dutch discovered the Kamojang geothermal field in 1920 and began in 1973 with the Indonesian Government and New Zealand cooperation. After ten years of exploration, in 1983, this field was able to produce 140 MWe, and in 1997 expanded to 220 MWe [9].

A hypothesis in this study is that the Kamojang geothermal field is a caldera system with several composite cones of andesitic volcanoes. The reservoir Well C-1 is rock-dominant. A condensate layer with a value of oxygen atom fraction in rock greater than that of the upper reservoir layer is located above the reservoir layer.

A. Geological Regional of Kamojang Geothermal Field

The research area is part of the western Indonesia. It is influenced by tectonic activity in the form of subduction between the Eurasian Continental Plate and the Indian – Australian Ocean Plate [10], which has been going on since the Eocene Period and is still ongoing today. The collision is oblique subduction on the Sumatra Island and produces a long-dimensional horizontal fault system known as the Sumatra Fault [11]. Meanwhile, in Java, the collision between these plates is frontal/perpendicular subduction, and there is no horizontal fault system in long dimensions such as the Sumatra Fault. Therefore, the island of Java seems to have a simple structure that displays the expression of the physiographic zone trending east-west, which is, of course, related to its structural control [12]-[14].

According to [15], the alignment pattern of the geological structure of Java Island can be divided into 3 (three) straightness directions: Meratus Pattern trending northeast-southwest, Sunda Pattern trending north-south, and Java Pattern trending west-east. As explained in [16], the results of this subduction in Java form a magmatic arc from the Late Eocene to the Quaternary with magmatism affinity resulting from tholeiitic, medium-high calc-alkali to shoshonitic.

The West Java Kamojang geothermal field is included in the Quaternary age magmatism arc with a calk-alkaline magma affinity. According to [5] in West Java, the highest identified geothermal field population is forty prospect areas (Figure 1).

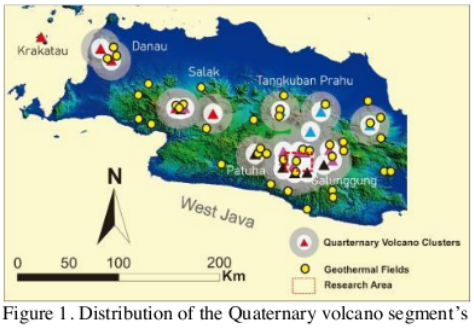

Figure 1. Distribution of the Quaternary volcano segment's boundary zone in West, Central, and East Java Island (Modified from [5])

However, the potential and geothermal producers are only in the two grouped areas: the Salak zone (Awi Bengkok) and the Galunggung-Tangkuban Prahu zone (Kamojang, Darajat, and Wayang Windu). The Galunggung-Tanggkuban Prahu zone is located around the Quaternary volcanic cone cluster, namely the Kendang volcanic complex [17]. This volcanic cone is located inside an old caldera called the Pangkalan caldera, which is Pleistocene.

According to [18], the Kamojang geothermal field is located in a series of large volcanoes lined up from the west towards the east, covering: Mt. Rakutak, Ciharus Lake, Pangkalan Lake, Mt. Gandapura, Mt. Guntur, and Mt. Masigit. The series of the volcanos are aged from 1.2 to 0.452 Ma (K-Ar method) [19]-[20]. The analysis of the geochemical and petrographic of volcanic rocks showed that the Kamojang geothermal field is composed of basalt, andesite, and basaltic andesite [21]. In contrast, the up-flow geothermal area was located in the middle of Kamojang [22].

As suggested in [7] and [23], there were two hydrothermal mineral assemblages present, namely those produced by 'acid' and 'neutral' pH fluids. The alteration zone in Kamojang geothermal field can be divided into argillic and propylitic zones [24]. The argillic zone was dominated by clay minerals consisting of kaolin (< 120°C), smectite (< 150°C), and smectite-illite (> 200°C) formed in acidic conditions near neutral (steam zone).

The propylitic zone is an assemblage of minerals at a more in-depth level, and it has a temperature above 200°C in the reservoir zone. Minerals present in this zone are epidote, adularia, wairakite, non-swelling chlorite, and calcite. [25] researched at KMJ-48 and KMJ-53 wells and found the high-temperature minerals, namely wairakite, illite, and epidote. These minerals have a range of about 250°C, and the temperature measured in the well is 245°C. Adularia indicates high permeability in core samples of well KMJ-53 (710-712 m, 992-996 m) and KMJ-48 (819-821 m and 1372-1375 m).

The quartz thermo-luminescence analysis shows the old heat flows from the lower KMJ-10 well [26]. This heat was interpreted as derived from the older igneous intrusion. The heat source under KMJ-78 and CHR-1 wells were construed as coming from the young intrusive rocks.

II. METHODS

A. Study Area

Physiography is the physical form of the appearance of the earth surface. The shape of the earth surface is closely related to the earth dynamics, caused by both endogenous and exogenous processes. The Kamojang area is physiographically included in the Quaternary volcanic zone. In this zone, volcanoes grow up to 1500 m in height, stretching from west to east from Mount Rakutak to Mount Guntur in the east. The area is located in the West Java province, approximately 60 miles from Bandung to the southeast. The place can be reached from Garut, continued to the north about 21 km. The Kamojang crater is the tourism area (Figure 2). Several volcanoes grow in the Kamojang geothermal field, such as: Mt. Rakutak, Mt. Gandapura, Mt. Cakra, Mt. Sanggar, Mt. Pasir Jawa and Ciharus Lake, Mt. Jawa and Mt. Guntur.

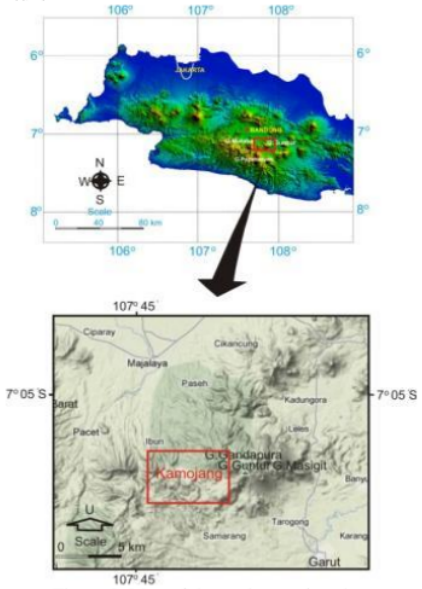

Figure 2. Map of the study area location

B. Analysis Tools

This study aims to study the physical characteristics of the geothermal field reservoir

rock, especially the C-1 well, using ^{18}O isotope analysis of the alteration rock. Knowing the rock properties of the reservoir rock, the type of geothermal system in the Kamojang field can be identified, whereas previous studies used hydrothermal fluid isotope analysis. It is hoped that the ^{18}O isotope analysis method from alteration rock can reduce exploration costs because there is no need to take hydrothermal fluid from the well. This method requires laboratory analysis, such as petrographic analysis using thin sections and X-ray diffraction (XRD). Both methods are used to identify primary and secondary mineral types from rocks.

Meanwhile, ^{18}O isotope analysis is used to determine the ^{18}O isotope composition of the alteration rock. The ^{18}O isotope analysis used the Isotope Ratio Mass Spectrometer (IRMS) method. Rock samples taken were nine samples of alteration rock from Sumur-C1 with seven samples for petrographic analysis, nine samples for X-ray diffraction, and three samples for ^{18}O isotope analysis. Apart from using several laboratory analytical methods, this study also uses secondary data obtained from the literature. Meanwhile, basic knowledge about the 18O isotope uses several chemical equations, which are described as follows.

One of the basic concepts used in stable isotopes, such as isotopes of hydrogen, carbon, nitrogen, oxygen, and sulfur, interprets the geological and environmental processes. Thus, $\delta^{18}O$ and δD analysis was conducted to identify meteoric isotope water in certain areas and use the information to study water evolution [27]-[28]. The research was usually displayed on a plot of two isotopes. Meteoric water was located along a straight line in equation 1 given in [29], [30]:

$$\delta D = 8\ \delta^{18}O + 10 \text{ [29], [30]} \quad (1)$$

Research on stable isotopes between minerals and fluids has expanded rapidly in geochemical development [31]-[32] because it can solve problems by using the interpretation of isotope geology. Thus, as explained in [33] and [34], the oxygen isotope fractionation between rock and fluids can be assumed as the relationship of smectite-H_2O. The plagioclase feldspar (An_{30}) - H_2O relationship was assumed in [35]-[38], while the muscovite-H_2O relationship was argued in [39]. The stable isotope fractionation between minerals was studied by conducting a series of experiments on isotope exchange between plagioclase (Ab) and water (H_2O) [40]. The following formula gave the experimental results:

$$100 \ln \alpha Ab\text{-}H_2O = 2{,}39 \times 106T\text{-}2 - 2{,}51 \quad (2)$$

where T is in Calvin. The exchange reaction of oxygen isotope between rock and fluids can be considered as a simple water-rock interaction. As explained in [33], the rock $\delta^{18}O$ value changes, resulting in the interaction between the water-rock, to obtain the final isotopic composition of rocks (δ^{r}_{f}) and the end of the isotopic composition of water (δ^{w}_{f}). The end of the isotopic composition of rocks (δ^{f}_{r}) was embodied in the following equation:

$$\delta^{r}_{f} = \delta^{r}_{i} + x[1000 \ln \alpha Ab\text{-}H_2O + (\delta^{w}_{i} - \delta^{r}_{i})], \quad (3)$$

While the final isotopic composition of water (δ^{f}_{w}) was expressed in the equation:

$$\delta^{w}_{f} = (\delta^{r}_{i} - 1000 \ln \alpha Ab\text{-}H_2O)\ (1\text{-}x) + x(\delta^{w}_{i}) \quad (4)$$

where i is the initial state (i.e., before the water-rock interactions), whereas f is the final state (i.e., after the water-rock interaction), w is water, and r is the rock. X was a fraction of the oxygen atoms in the water system, while $1\text{-}x$ is a fraction of the oxygen atoms of rocks in the system.

III. Result and Discussion

A. Geology of Kamojang Geothermal Field

The regional stratigraphy of the research area is part of the West Java stratigraphy that was suggested by [41]. In this stratigraphic unit, the West Java area can be divided into three sedimentation units. The sedimentation units were Continental Shelf Unit, including Jakarta-Cirebon Block; Bogor Basin Unit, including Bogor Block and Southern Mountains and the western part, are Banten Unit, which includes the following: Banten Block. Meanwhile, the stratigraphy of the research area is included in the Bogor Basin. The Bogor Basin is characterized by gravitational flow deposits in the form of igneous and sedimentary rock fragments such as andesite, basalt, tuff, and limestone with an estimated thickness of more than 7,000 meters. The youngest rocks from the Bogor Basin are volcanic deposits. The structure and tectonics that affect the Kamojang area are the low Caldera Pangkalan, normal faults trending northwest-southeast and faults trending north-south [18]. The Caldera Pangkalan is represented by a sharp wall located in the west; meanwhile, the northwest-southeast normal fault is located in the northern part of Kamojang, while the north-south pattern is located in the eastern part, where there is an alignment of surface manifestations.

Following the geological setting from [24], the research area can be divided into several rock units: Pre-caldera Volcanic Stratigraphic Unit and Post-Caldera Volcanic Stratigraphic Unit.

Pre-caldera volcanic stratigraphic units consist of Mount Sanggar Volcanic Rocks, Mount Ciharus Volcanic Rocks, Mount Jawa Volcanic Rocks, Mount Beling Volcanic Rocks, and Pasir Jawa Volcanic Rocks. In contrast, the post-Caldera stratigraphic unit consists of Mount Cakra Volcanic Rocks (Figure 3). The discussion regarding the sequence of the stratigraphic units in the study area from old to young can be followed like this:

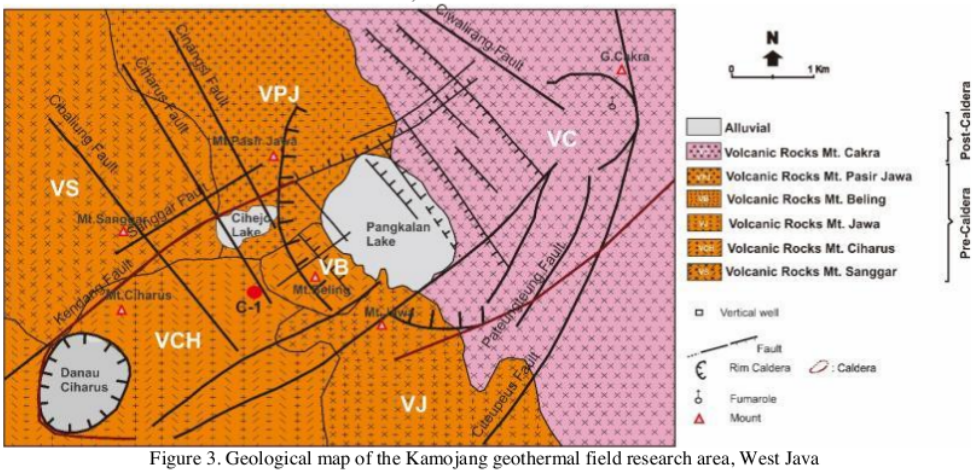

Figure 3. Geological map of the Kamojang geothermal field research area, West Java

1) Mount Sanggar Volcanic Rocks.

This rock unit forms a volcanic cone, as seen in Figure 3. The rock unit consists of andesite lava and pyroclastic fall deposits (scoria fall); an outcrop photo can be seen in Figure 4. Andesite lava exhibits massive, porphyritic, and hypocrystalline textures. With a plagioclase phenocryst, pyroxene, embedded in the base mass of volcanic glass. The pyroclastic fall deposits show a multi-layered structure. They are composed of ash-lapilli size, andesite scoria embedded in volcanic ash, with a thickness of this outcrop of about 35 cm. Volcanic Rock Unit Mount Sanggar is a rock unit from the Kamojang caldera system. The Mount Sanggar volcanic rocks unit is present at around an elevation of 1300 m and extends from the west and deeper towards the north. The distribution of these rock units can be seen in Figure 3.

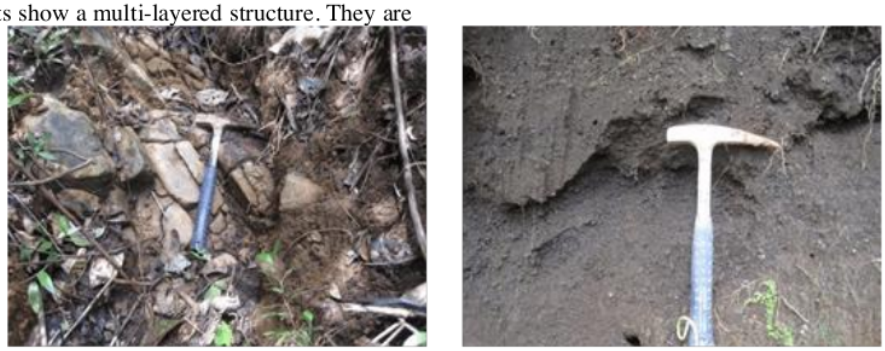

Figure 4. Andesite lava outcrops and pyroclastic fall deposits from the Mount Sanggar Volcanic Rock Unit. The pyroclastic fall deposits show a multi-layered structure. The grain size is ash-lapilli size, composed of andesite scoria embedded in volcanic ash

2) Mount Ciharus Volcanic Rocks

This volcanic unit is a form of negative morphology, a lake surrounded by hills from Mount Ciharus. The rocks that make up the morphology are andesite lava and pyroclastic breccia deposits that fall out on the edge of the lake. The pyroclastic fall breccia deposits showing a multi-layered structure. The grain size is an ash-lapilli size, composed of andesite fragments scoria embedded in volcanic ash. This andesite lava has a massive, hypocrystalline porphyritic structure. With a plagioclase phenocryst, pyroxene is embedded in the glass volcanic ground mass. In contrast, the subsurface lithologies consist of andesitic lava, andesite breccia, and andesite tuff. This rock unit spreads only in the southwestern part of the study area at an elevation of 800–1200 m.

3) Mount Jawa Volcanic Rocks

These rock units form volcanic cone

morphology. The cone is composed of andesite lava and pyroclastic fall deposits (Figure 5). Andesite lava exhibits a massive, hypocrystalline porphyritic structure. The plagioclase and pyroxene were as phenocryst embedded in volcanic glass as ground mass. Pyroclastic fall deposits show a multi-layered structure. The grain size of pyroclastic fall was ash-lapilli. And fragments composed of andesite scoria embedded in volcanic ash. Under this rock surface, the unit comprises andesite lava, andesite breccia, and andesite tuff. These rock units spread only in the southeastern part of the study area, an elevation of 1600–700 m.

Figure 5. Outcrop of pyroclastic fall deposits and andesite lava from Mount Jawa. The pyroclastic fall deposits show a multi-layered structure. The grain size is ash-lapilli and fragments, composed of andesite scoria embedded in volcanic ash

4) Mount Beling Volcanic Rocks

This lithology unit forms volcanic cones' morphology. The lithology comprises pyroclastic fall deposits showing a multi-layered structure in ash-lapilli size (Figure 6). The fragments consist of andesite with structure scoria embedded in volcanic ash, the thickness of this outcrop is about 10-50 cm, and some outcrops are more than 1 m. Below the surface, rock units spread around Mount Beling and are at an elevation of 1500–1400 m.

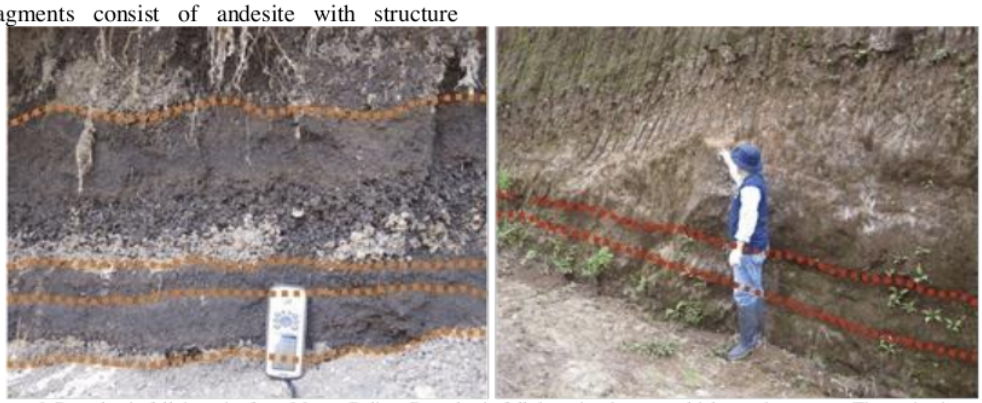

Figure 6. Pyroclastic fall deposits from Mount Beling. Pyroclastic fall deposits show a multi-layered structure. The grain size was ash-lapilli, and fragments consisting of andesite with structure scoria embedded in volcanic ash

5) Pasir Jawa Volcanic Rocks

The morphology of these rock units forms volcanic cones. The lithological units of the cone consisting of andesite lava and falling pyroclastic deposits (Figure 7). Lava shows a massive structure and hypocrystalline porphyritic texture. Meanwhile, plagioclase and pyroxene are present as phenocrysts embedded in the ground mass of volcanic gases. Falling pyroclastic deposits show a multi-layered structure. The grain size is lapilli ash, and the fragments consist of scoria andesite embedded in volcanic ash. The subsurface rock units were composed of andesite lava, andesite breccia, and andesite tuff. These rock units are scattered only in the western part of the study area at an elevation of 1600 - 600 m.

Figure 7. Andesite lava outcrop from Mount Pasir Jawa found in Curug Madi. Pyroclastic fall deposits show a multi-layered structure. The grain size is ash-lapilli size, and fragments are composed of andesite scoria embedded in volcanic ash

6) Mount Cakra Volcanic Rocks

The morphology of these rock units forms a volcanic cone. These rock units consist of andesite lava, pyroclastic fall deposits, and pyroclastic-flow deposits (Figure 8). Andesite lava has a massive, hypocrystalline porphyritic structure. With plagioclase phenocrysts, pyroxene was embedded in glass-based masses. Pyroclastic fall deposits show a multi-layered structure. Ash-lapilli size and consist of andesite fragments scoria embedded in volcanic ash. Pyroclastic flow deposits are found at the top of Mount Cakra, and these deposits contain charcoal (Figure 9). The age analysis results of wood charcoal sample are 0.002077 ± 0.000021 million (age dating using the method ^{14}C). It shows that the incidence of volcanic eruptions occurred at that age.

Pyroclastic flow deposits are poorly sorted. Ash-lapilli size and consist of andesite fragments scoria embedded in volcanic ash. The subsurface rocks unit was composed of andesite lava, andesite breccia, and andesite tuff. These rock units are scattered only in the eastern and southeastern parts of the study area at an elevation of 2000 - 400 m.

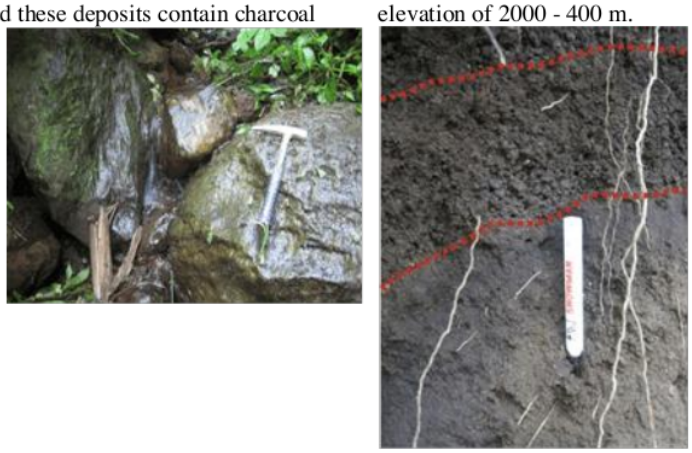

Figure 8. Pyroxene andesite lava outcrops and pyroclastic fall deposits from Mount Cakra. The pyroclastic fall deposits show a multi-layered structure. Ash-lapilli grain size and consists of andesite fragments scoria embedded in volcanic ash

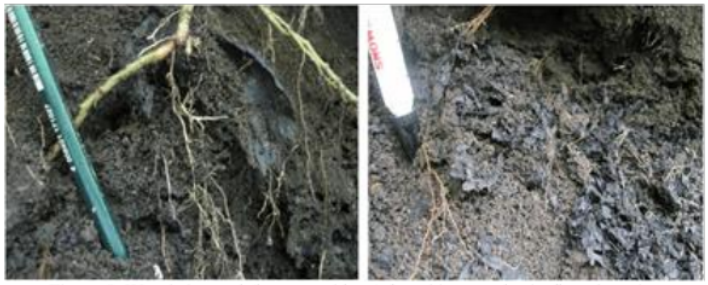

Figure 9. Wood charcoal (leaves and logs) found in pyroclastic-flow deposits

B. The Lithology of Well C-1

The research area is an area of the geothermal field, which consists of Quaternary volcanic rocks that have undergone hydrothermal alteration. The alteration rocks exposed around the Kamojang crater and well were also exposed along with some geothermal manifestations such as mud pool, steaming ground, fumarole, and hot spring. The andesite lava, pyroclastic fall, and pyroclastic flow breccia can be found in the crater wall.

In this study, the samples were obtained from the core and cutting well C-1 from shallow to depths (Figure 10). The rock samples were analyzed by petrographic and X-ray diffraction (XRD) methods. The petrographic samples were observed on both the texture and mineralogical composition. Lithological types can be followed as below:

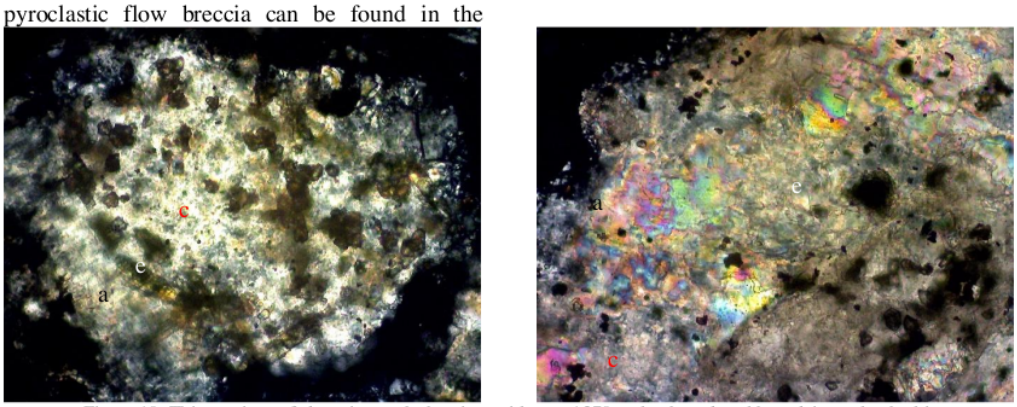

Figure 10. Thin sections of alteration rock showing epidote at 1370 m depth replaced by calcite and anhydrite

Tuff altered is present at shallow depths (0-50 m), fine to medium-grained (0.1 to 0.2 cm), composed of plagioclase, quartz in volcanic glass ground mass. These rocks altered weak (15%), consisting of montmorillonite, calcite, quartz, cristobalite, and hematite.

Andesite breccia altered was present at a depth of 50-250 m and 600 -1320 m, medium to coarse-grained (0.2 to 0.5 cm), composed of andesite, volcanic tuff in glass ground mass. Mineral alterations were illite-montmorillonite, quartz, chalcedony, chlorite, calcite, adularia, wairakite, epidote, hematite, and pyrite. Mineral alteration ranges from 30-80%.

Andesite lava altered was gray, fine to medium-grained (0.1 to 0.2 cm) with porphyritic texture. Phenocryst composed of plagioclase, pyroxene, and opaque minerals were embedded in ground mass volcanic glass. These rocks have experienced approximately 30-80% partial alteration. Meanwhile, the alteration minerals that exist are chlorite, quartz, cristobalite, amorphous silica, illite-montmorillonite, epidote, illite, wairakei, and iron oxide.

C. Alteration Mineralogy of Well C-1

Petrographic and XRD analysis was performed on nine samples in wells C-1 showing the presence of several secondary minerals that can be seen in Figures 10 and 11, and actualized in the composite log in Figure 12:

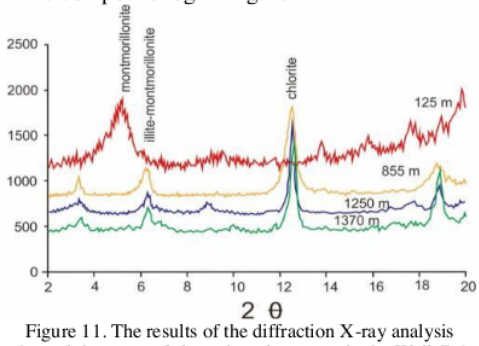

Figure 11. The results of the diffraction X-ray analysis showed the types of clay minerals present in the Well C-1

Cristobalite generally is present at shallow depths, i.e., <200 m depth. Cristobalite amounts to 3-15%, and these minerals replace most of the plagioclase and ground mass. *Quartz* is present in almost every depth, ranging between 5-45%. Some wells showed more abundant quartz with increasing depth. Quartz can be present to alter plagioclase, pyroxene, and ground mass and can occur as a mineral filler in veins and cavities. It can be present with calcite, anhydrite, epidote, wairakite, quartz, pyrite, and hematite as fillers of veins.

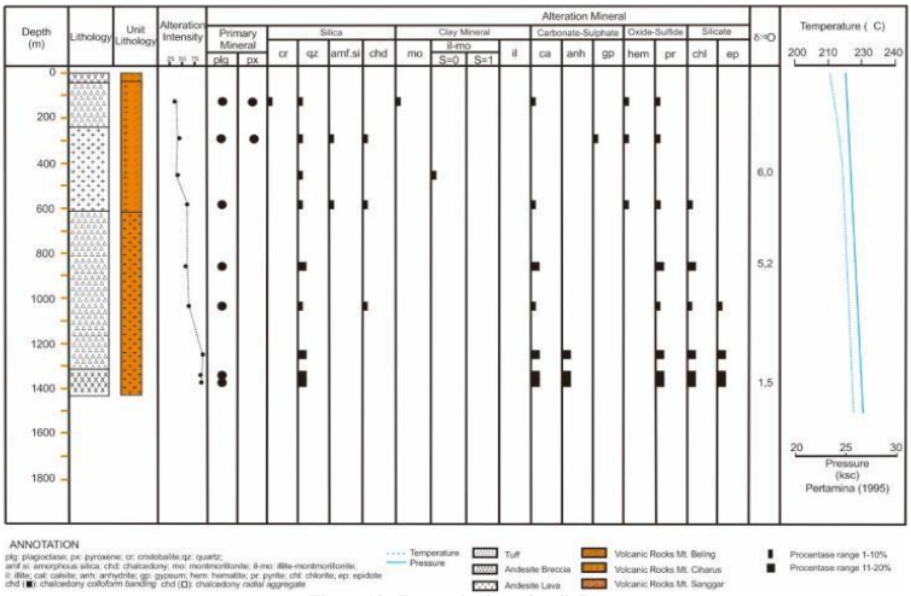

Figure 12. Composite log of well C1

Clay minerals were identified using the ethylene glycol of the X-ray diffraction method. In general, these clay minerals alter plagioclase, pyroxene, and ground mass. Attendance of some clay minerals included: montmorillonite at a depth 125 m, coming with cristobalite, quartz, calcite, hematite, and pyrite. Illite-montmorillonite; these minerals can be found at a depth of about 125-600 m. The mineral is present with anhydrite, calcite, quartz, pyrite, and hematite. In contrast, chlorite is present at depths > 600 m.

Calcite replaces plagioclase, pyroxene, and ground mass. Calcite also is present as mineral filler in veins and cavities. Calcite can be present with several minerals, i.e., quartz, epidote, wairakite, anhydrite, and pyrite. The presence of calcite ranges from 5-30%. This mineral is found in almost any depth.

Anhydrite was a mineral alteration replacing plagioclase, pyroxene, and ground mass. Apart from being a mineral alteration, it is also a mineral filler in crystal fracture, cavities, or veins, with calcite, chlorite, epidote, quartz, and wairakite. It was found to comprise less than 12% of the rock alteration at > 1300 m depth.

Chlorite was replacing plagioclase, pyroxene, and ground mass. In plagioclase and pyroxene, chlorite is replacing at the edges or in cleavage crystal. Apart from being an alteration mineral, chlorite is seen in some thin sections as a mineral filler in cracks, voids, or veins. It was also present with calcite, anhydrite, illite-montmorillonite, epidote, quartz, and wairakite. Attendance ranged between 5-35% in the rock alteration. Chlorite is present at depths > 600 m.

Epidote was present at a deeper depth, of approximately > 1000 m, replacing plagioclase and pyroxene. Most epidote filled veins with quartz, wairakite, chlorite, calcite, anhydrite, adularia, and pyrite. It was present as mineral alteration of about 8%. At several sites in the thin sections, epidotes were replaced by calcite and anhydrite (Figure 10).

Hematite partially replaced plagioclase, pyroxene, and ground mass. It can be present as filler mineral in veins and cavities with calcite, gypsum, quartz, chalcedony, amorphous silica, cristobalite, illite-montmorillonite, chlorite, pyrite, and calcite. Hematite is common in shallow depths, ranging between 3-12%.

Pyrite is present at almost any depth as a replacement of pyroxene and ground mass. It can be present as a mineral filler vein with calcite, gypsum, anhydrite, quartz, chalcedony, amorphous silica, illite-montmorillonite, chlorite, cristobalite, and calcite, epidote, adularia, and wairakite. The pyrite content ranges between 2-12%

D. Alteration Zone of Well C-1

The identification of mineral alteration at well C-1 showed that the hydrothermal alteration zones are cristobalite-montmorillonite, illite-montmorillonite, and chlorite-epidote. The interpretation of temperature mineral alteration of each zone (Table 1.) was based on [42], [43].

Table 1.
Mineral index temperature of well C-1

Minerals		Temperature 50	100	200	300°C
Primary	Minerals Plagioklas Groundmass				
Scondary	Quatrz				
	Crystobalite				
	Montmorillonite				
	Illite-Montmorillonite				
	Calcite				
	Anhydrite				
	Chlorite				
	Epidote				
	Hematite				
	Pyrite				
Alteration Zone		Crystobalite-Montmorillonite	Illite-Montmorillonite	Chlorite-Epidote	

The Cristobalite-montmorillonite zone is characterized by cristobalite, montmorillonite, quartz, calcite, anhydrite, gypsum, hematite pyrite. Minerals are present at <400 m depth, formed at temperatures below 100°C.

The second zone was the *Illite-montmorillonite zone*. This zone is characterized by illite-montmorillonite, calcite, anhydrite, gypsum, hematite, and pyrite. The secondary minerals of this zone are present at a range from 500-1000 m depth. The temperature of this zone ranged within about 100-200°C. The zone is determined based on the formation of cristobalite and montmorillonite minerals.

The next zone is the deepest, namely the *Chlorite-Epidote zone*. This zone is characterized by the appearance of chlorite, epidote, wairakite, hematite, and pyrite. Minerals are present at > 1000 m depth. The temperature of this zone is based on the formation of chlorite and epidote. The minerals were formed at temperatures higher than 200°C. This zone is the reservoir, with temperatures ranging from 235-250°C [44].

E. Isotope Water and Alteration Rocks

1) Isotope Meteoric Water of Kamojang Geothermal Field

Measurement of isotope meteoric water of Kamojang geothermal field was done in [45], [46]. The isotope measurements include measurement of isotopes ^{18}O and D of the water manifestations, rainwater, and shallow well water. Isotope measurements on the surface manifestation are situated at an elevation of about 1500 m. They were indicating that the $\delta^{18}O$ value around -8.40 to -8.50 ‰, while the δD value of approximately -48.60 to -50.10 ‰. The $\delta^{18}O$ rainwater measurements of Kawah 1 and Lab. K.M.J. (II) from October to March showed an average value for $\delta^{18}O$ around -7.50 to -7.78 ‰, and δD value approximately -43.32 to -45.42 ‰. The results of plotting $\delta^{18}O$ and δD value of samples obtained in the diagram of variation $\delta^{18}O$ and δD indicate that all water samples were at the meteoric water line. It means that the hydrothermal fluid origin affecting the Kamojang geothermal field system is meteoric water (Figure 13).

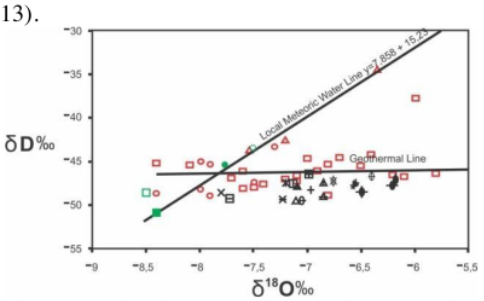

Figure 13. A plot of oxygen and deuterium isotope samples of rainwater, manifestation, and the Kamojang geothermal field [45], [46]

2) Oxygen Isotope Alteration Rock.

Isotopes were an artifact. Studying the abundance of stable isotopes in the geological environment is very important. It aims to explain the background and environmental perspectives, such as mineral deposits, plutonic phase, sediment formation, deposition conditions, and rock age. Therefore, isotopes ^{18}O and D can be used to study the relationship of fluids and minerals in the hydrothermal system. As explained in [48]-[50], the isotope ^{18}O to ultramafic rocks ranges within > 5 and <7 ‰. Basalt and gabbro account for ≈5.5 to <8 ‰, while andesite and granodiorite makes from ≈5.5 to > 12 ‰. According to [51], andesite has a value of + 6.0 ‰ $\delta^{18}O$. Rhyolite and granite have a value of ≈6 to 13 ‰. In calculating the water-rock ratio in this study for the magmatic rocks, ^{18}O isotope values using the value of +6.0 ‰ of andesite proposed by [51]-[52]. Rhyolite and granite have a value of ≈6 to 13 ‰. Calculation of the water-rock ratio in this study resulted in the value of isotope ^{18}O magmatic rocks using +6.0 ‰ of andesite, as proposed by [51].

The ^{18}O isotopic analysis of alteration rocks was done to three samples from shallow to depths. This sample represents the argillic, illite-montmorillonite, and chlorite-epidote zones. The samples analyzed were taken at 456 m, 855 m, and 1370 m depth. Results of isotope ^{18}O analysis of the three samples successively were 6.0, 5.2, and 1.5 ‰. This analysis indicates that towards the depth, the content of isotopes ^{18}O of alteration rock was getting low. This value gives the sense that $\delta^{18}O$ content in altered rocks at shallow depths is contained by a weak alteration-not modified, while at depths in $\delta^{18}O$ contained by strongly altered rock. This value was caused by the interaction of rocks with hydrothermal fluids.

F. Water-Rock Interaction

1) Final Rock Isotope Composition (δ^{r}_{f})

While determining the isotopic composition (δ^{r}_{f}) in the final rocks, it was necessary to use data regarding the type of rock, calculation of relationships of mineral-H_2O system (Equation 3), initial isotopic rocks, and water. X was a fraction oxygen atom of water in the system. And the value of 0, 0.25, 0.50, 0.75, and 1, and calculated at a temperature of 25° to 300°C. Isotopic ^{18}O compositions initial rock (δ^{r}_{i}), using the composition of andesite with a value of +6.0 ‰ [51], whereas the initial isotopic water (δ^{w}_{i}) using the average composition of isotope ^{18}O rainwater and Kamojang geothermal field manifestations was 8.05 ‰. Using equations 3 and 4, the following calculation results were obtained, as presented in Figures 14 and Table 2. Based on the analysis results, the value fraction oxygen atoms of water (x) obtained from the calculation range from 0.03 to 0.63. This value shows that the water-rock ratio of the geothermal system ranges from 3-63% or rocks-dominated system.

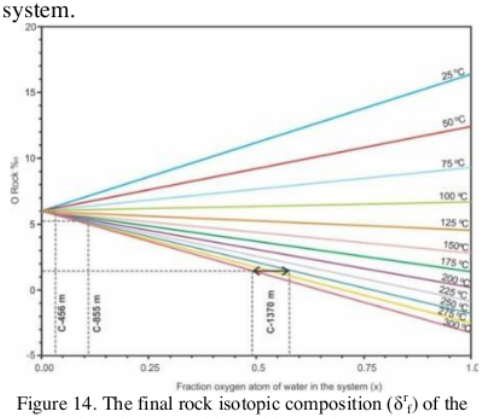

Figure 14. The final rock isotopic composition (δ^{r}_{f}) of the sample well C-1 at 456 m, 855 m, and 1370 m depth

Table 2.
Calculation results of the isotopic composition (δ^{r}_{f}) of final rocks, x is the fraction of the oxygen atoms of water in the system

Well	Depth (m)	$\delta^{18}O$ (‰)	T (C)	X
C-1	456	6.0	125	0.03
	855	5.2	225	0.12
	1370	1.5	250	0.48-0.63

2) Final Water Isotope Composition (δ^{w}_{f})

Final water isotopic composition (δ^{w}_{f}) was obtained from the following data: rock types, counting relations of mineral-H_2O system (Equation 3), initial isotopic of rock and water. 1-x as a fraction oxygen atom of rocks in the system with a value of 0, 0.25, 0.50, 0.75, and 1. The calculated temperature ranged within 25° to 300°C. ^{18}O isotopic compositions of initial rock (δ^{r}_{i}) used ^{18}O isotopic composition from andesite +6.0 ‰ [51], whereas the initial isotopic water (δ^{w}_{i}) showed the common isotope 18O composition of rainwater and Kamojang geothermal field manifestations, i.e., 8.05 ‰. Using equations 3 and 4, the obtained value of the fraction of oxygen atoms in the rock (1-x) is 0.16 or 16% (Table 3).

Table 3.
Isotopes of oxygen and deuterium, the temperature of well fluids, and the fraction oxygen atom of rock in the system (1-x). Data ^{18}O, D, and temperature were obtained from [45], [46]

Well	^{18}O (‰)	D (‰)	T (C)	(1-x)
CHR-1	-6.50	-48.30	228.80	0.16

According to [31], the water-rock ratio value is around <0.2 or <20%. The ratio indicates that this rock-dominated system is not fluid. Thus, according to these calculations, it can be stated that the fluid reservoir in the well C-1 is 16%, and the system is rock-dominated (Figure 15).

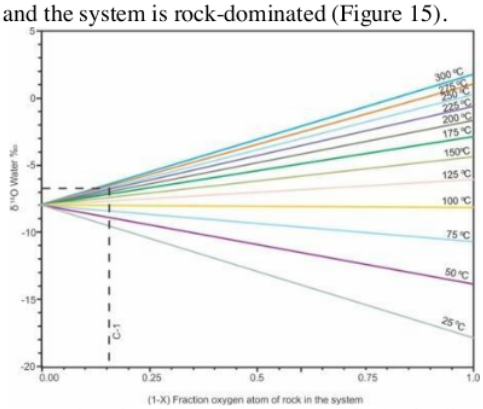

Figure 15. A plot of sample isotope oxygen fluids of well C-1 on the diagram fraction oxygen atoms of rocks in the system, the obtained value of the fraction oxygen atoms of rocks in the system (1-x)

IV. Conclusion

The Kamojang geothermal field is located in a caldera system in which several composite cone andesite volcanoes grow.

The ^{18}O and deuterium isotope analysis results showed that the water that goes into the Kamojang geothermal system is meteoric water. Isotope meteoric water has a content of around -8.05 ‰ $\delta^{18}O$ and δD approximately -46.86 ‰. The water entered into rocks and interacted with rocks to reach the reservoir as a fluid reservoir. The isotope ^{18}O explained that the reservoir's water-rock ratio in Well C-1 shows that the system is rocks-dominated. Because it has a value of fraction oxygen atom of rocks in the system (1-x) is 0.16 or fluids contained by the system is 16%. It was also seen in the thin

section. The veins and cavities are in a permeability zone. Now, veins are filled with secondary minerals, such as quartz, calcite, adularia, anhydrite, chlorite, epidote, and wairakite. The upper part of the reservoir zone is a condensate layer, with the value of fraction oxygen atom in the rock (x) ranging from 0.03 to 0.63, or 3-63%. This zone is characterized by the presence of montmorillonite, illite-montmorillonite, and chalcedony.

ACKNOWLEDGMENTS

We would like to thank Pertamina Geothermal Energi (PGE), Akita University, and the 2011 Sandwich Program of the Ministry of Education. We are also grateful for the 2016 Competitive Grants Program of the Ministry of Education for providing facilities for field mapping. And we express our unforgettable gratitude to the Petrographic Laboratory of the Department of Geological Engineering, UPN "Veteran" Yogyakarta, which has provided facilities.

REFERENCES

[1] IBRAHIM, R. F., FAUZI, A., & SURYADARMA. (2005) The Progress of Geothermal Energy Resources Activities in Indonesia. *Proceedings World Geothermal Congress Antalya, Turkey,* pp. 1-7. https://www.geothermal-energy.org/pdf/IGAstandard/WGC/2005/0142.pdf

[2] WAHYUNINGSIH, R. (2005) Potensi dan Wilayah Kerja Pertambangan Panas Bumi di Indonesia. *Colloqium*, *Field Investigation Results, the Directorate of Mineral Resources Inventory of Indonesia, Bandung, (in Indonesian with English abstract)*. http://psdg.bgl.esdm.go.id/kolokium/Makalah%20Umum/1.%20Makalah%20PB%20Potensi%20dan%20WKP%20Panas%20Bumi.pdf

[3] DEON, F., FÖRSTER, H. J., BREHME, M., WIEGAND, B., *et al*. (2019) Geothermal exploration in Indonesia based on Mineralogy and Hydrothermal Alteration. *I.O.P. Conference Series: Earth and Environmental Science*, 254(1), doi: 10.1088/1755-1315/254/1/012002.

[4] SURYANTINI, SETIJADJI, L.D., WAHYUNINGSIH, R., EHARA, S., *et al*. (2005). Geothermal Fields of Java Island, Indonesia: Their Descriptions, Geologic Environments, and Preliminary Area-Selection Exploration Strategy. *Proceedings of the 3rd International workshop on Earth Science and Technology, Kyushu University, Fukuoka*, pp.11-18.

[5] SETIJADJI, L.D. (2010) Segmented Volcanic Arc and its Association with Geothermal Fields in Java Island, Indonesia. *Proceedings World Geothermal Congress, Bali, Indonesia*, pp.1-12.

[6] MARLIYANI, G. I., HELMI, H., ARROWSMITH, J.R., CLARKE, A. (2020) Volcano morphology as an indicator of stress orientation in the Java Volcanic Arc, Indonesia. *Journal of Volcanology and Geothermal Research*, 400, article ID 106912, doi: 10.1016/j.jvolgeores.2020.106912,

[7] UTAMI, P. (2000) Characteristics of The Kamojang Geothermal Reservoir (West Java) as revealed by its Hydrothermal Alteration Mineralogy. *Proceedings of the World Geothermal Congress*, pp. 1921–1926. Available at: http://web01.opencloud.dssdi.ugm.ac.id/wp-content/uploads/sites/395/2012/12/Characteristics-of-the-Kamojang-Geothermal-Reservoir-2000-Pri-Utami.pdf.

[8] KAMAH, M. Y., DWIKORIANTO, T., ZUHRO, A. A., SUNARYO, D., & HASIBUAN, A. (2005) The Productive Feed Zones Identified based on Spinner Data and Applications in the Reservoir Potential Review of Kamojang Geothermal Area, Indonesia. *Proceedings of the World Geothermal Congress*, *Antalya, Turkey,* pp. 1-6.

[9] SUDARMAN S, BOEDIHARDI, M., PUDYASTUTI, K., & BARDAN. (1995) Kamojang Geothermal Field 10 Year Operation Experience. *Proceedings World Geothermal Congress*, pp.1773-1777.

[10] PENA-CASTELLNOU, S., INDAH MARLIYANI, G. & REICHERTER, K. (2019) Preliminary Tectonic Geomorphology of the Opak Fault System, Java (Indonesia). *Eguga*, 21, pp. 12307. Available at: https://meetingorganizer.copernicus.org/EGU2019/EGU2019-12307.pdf.

[11] SIEH, K., & NATAWIDJAJA D. (2000) Neotectonics of the Sumatran Fault, Indonesia. *Journal of Geophysical Research*,

105(B12), pp. 28295-28326.
[12] HALL, R., CLEMENTS, B., SMYTH, H. R., & COTTAM, M. A (2007) A new interpretation of Java's structure, *Proceedings of Indonesian Petroleum Association*, pp. 1-23. Available at: http://searg.rhul.ac.uk/pubs/hall_etal_2007 Java Structure_IPA.pdf.
[13] AHNAF, J. S. PATONAH, A., PERMANA, H., & ISMAWAN, I. (2018) Structure and Tectonic Reconstruction of Bayah Complex Area, Banten. *Journal of Geoscience, Engineering, Environment, and Technology*, 3(2), pp. 77. DOI: 10.24273/jgeet.2018.3.2.1554.
[14] HARYANTO, I., ILMI, N. N., HUTABARAT, J., ADHIPERDANA, B.G., *et al*. (2020). Tectonic and geological structures of Gunung Kromong, West Java, Indonesia. *International Journal of GEOMATE*, 19(74), pp. 185–193. DOI: 10.21660/2020.74.05449, https://www.geomatejournal.com/sites/default/files/articles/185-193-05449-Iyan-Oct-2020-74.pdf
[15] PULUNGGONO & MARTODJOJO S. (1994) Perubahan Tektonik Paleogen-Neogen Merupakan Peristiwa Tektonik Terpenting di Jawa. *Proceedings Geologi dan Geotektonik Pulau Jawa Sejak Akhir Mesozoik Hingga Kuarter,* pp. 1-14.
[16] SOERIA-ATMADJA, R., MAURY, R. C, BELLON, H., PRINGGOPRAWIRO, H., *et al*. (1994) Tertiary Magmatic Belts in Java. *Journal of Southeast Asia and Petrology*, 9, pp. 13-27,
[17] REJEKI, S., HADI, J., & SUHAYATI, I. (2005). Porosity Study for Detail Reservoir Characterization in Darajat Geothermal Field, West Java, Indonesia. *Proceedings of the World Geothermal Congress 2005, Antalya, Turkey*, https://www.geothermal-energy.org/pdf/IGAstandard/WGC/2005/0634.pdf
[18] ROBERT, D. (1988) Subsurface Study on the Optimization of the Development of the Kamojang Geothermal Field. BEICIP/ GEOSERVICES Report for Pertamina, pp. 47.
[19] ROBERT, D., RAHARSO R, & BASTAMAN S. (1983) Exploration and Development of the Kamojang Geothermal Field. *Proceedings of the Indonesian Petroleum Association,* 1, pp. 171 – 190.
[20] ROBERT, D. (1987) Geological Study of the Western Part of the Kawah Kamojang Geothermal, PERTAMINA/BEICIP report, pp. 89.
[21] YUDIANTORO, D. F., SUPARKA, E., TAKASHIMA, I., ISHIYAMA, D., KAMAH, Y. (2012) Alteration and Lithogeochemistry of Altered Rocks at Well KMJ-49 Kamojang Geothermal Field, West Java, Indonesia. *International Journal of Economic and Environment Geology,* 3(2), pp. 21–32.
[22] YUDIANTORO, D. F., SUPARKA, E., YUWONO, S., TAKASHIMA, I., *et al*. (2013) Interstratified Illite/Montmorillonite in Kamojang Geothermal Field Indonesia. *Indonesian Journal of Geology, Geological Agency*, 4, pp. 177-183, http://ijog.bgl.esdm.go.id/index.php/IJOG/article/view/167/167
[23] UTAMI, P. R. I. ; BROWNE, P. R. L. (1999) Subsurface Hydrothermal Alteration in The Kamojang Geothermal Fields, West Java, Indonesia. *Proceedings Twenty-Fourth Workshop on Geothermal Reservoir*, Stanford University, Stanford California. Available at https://citeseerx.ist.psu.edu/viewdoc/download?doi=10.1.1.545.7179&rep=rep1&type=pdf
[24] KAMAH Y., TAVIP D. & AGUS A. Z. (2003) Penanggulangan Problem Geologi Dalam Operasi Pemboran Sumur Di Blok Timur Area Geothermal Kamojang Jawa Barat Indonesia. *Proceedings 6Th Indonesian Geothermal Association*, pp. 175-184.
[25] PURBA, S. (1994) Hydrothermal Alteration of Core and Cutting Samples from Wells KMJ-48 and 53 Kamojang Geothermal Field West Java Indonesia, pp. 58, unpublished.
[26] SUPARKA, K., YUDIANTORO, D. F., TAKASHIMA, I., HUTABARAT, J., & KAMAH, M. Y. (2013) Current Temperature Studies in Kamojang Geothermal Field West Java Indonesia. *Proceedings of the 2nd ITB Geothermal Workshop 2013 Institut Teknologi Bandung, Bandung, Indonesia*, pp. 1–8. Available at: http://eprints.upnyk.ac.id/12123/

[27] YU, X., LIU, C., WANG, C., ZHAO, J.-X., & WANG, J. (2021) Origin of geothermal waters from the Upper Cretaceous to Lower Eocene strata of the Jiangling Basin, South China: Constraints by multi-isotopic tracers and water-rock interactions. *Applied Geochemistry*, 124, article ID 104810, doi: 10.1016/j.apgeochem.2020.104810

[28] BLASCO, M., AUQUE, L. F., GIMENO, M. J., ACERO, P., ASTA, M. (2017) Geochemistry, geothermometry and influence of the concentration of mobile elements in the chemical characteristics of carbonate-evaporitic thermal systems. The case of the Tiermas geothermal system (Spain). *Chemical Geology,* 466(May), pp. 696–709, doi: 10.1016/j.chemgeo.2017.07.013,

[29] CRAIG, H. (1961) Isotopic variations in meteoric waters. *Science*, 133(3465), pp. 1702–1703, doi: 10.1126/science.133.3465.1702

[30] CRAIG, H. (1966) Isotopic composition and origin of the Red Sea and Salton Sea geothermal brines. *Science*, 154(3756), pp. 1544–1547, doi: 10.1126/science.154.3756.1544,

[31] RICHARDSON, S. M., & MCSWEEN, H. Y. JR. (1989) *Geochemistry Pathways and Processes*. Prentice Hall, pp. 208-235.

[32] MICHELSEN, N. (2020) Isotopic, chemical, and crowdsourcing studies of selected water cycle components in arid environments. Available at: http://tuprints.ulb.tu-darmstadt.de/17657/

[33] FIELD, C. W., & FIFAREK, R. H. (1985) Light Stable-Isotope Systematics in the Epithermal Environment. In BERGER, B.R. & BETHKE, P.M. (Eds.). *Geology and Geochemistry of Epithermal Systems, Reviews in Economic Geology, 2, Society of Economic Geologists,* pp. 99-128,

[34] CATHLES, L. M. (1983) An Analysis of the Hydrothermal System Responsible for Massive Sulfide Deposition in the Hokuroku Basin of Japan. In OHMOTO, H., and SKINNER, B. J. (Eds.). *The Kuroko and Related Volcanogenic Massive Sulfide Deposits: Economic Geology, Monograph* 5, pp. 439-487.

[35] TAYLOR, H. P. (1974) The application of oxygen and hydrogen isotope studies to problems of hydrothermal alteration and ore deposition. *Economic Geology*, 69(6), pp. 843–883, doi: 10.2113/gsecongeo.69.6.843,

[36] TAYLOR, H.P., JR. (1979) Oxygen and Hydrogen Isotope Relationships in Hydrothermal Mineral Deposits. In BARNERS, H.L. (Ed.). *Geochemistry of Hydrothermal Ore Deposits, Second Edition, John Wiley and Sons, New York*, pp. 236-277,

[37] OHMOTO, H., & RYE, R. O. (1974) Hydrogen and Oxygen Isotopic Compositions of Fluid Inclusions in the Kuroko Deposits. *Japan: Economic Geology,* 69, pp. 947-953.

[38] GREEN, G. R., OHMOTO, H., DATE, J., & TAKAHASHI, T. (1983) Whole-rock Oxygen Isotope Distribution in the Fukazawa-Kosaka area, Hokuroku district, Japan, and its potential application to mineral exploration. *Economic Geology*, 75, pp. 395-411.

[39] SPOONER, E.T.C., BECKINSALE, R.D., ENGLAND, P.C., & SENIOR, A. (1977) Hydration, ^{18}O Environment and Oxidation During Ocean Floor Hydrothermal Metamorphism of Ophiolite Metabasic Rocks from E. Liguria, Italy. *Geochemica et Cosmochimica Acta*, 41, pp. 857-871,

[40] MATSUHISA, Y., GOLDSMITH, J. R., & DAN CLAYTON, R. N. (1979) Oxygen Isotopic Fractionation in the System Quartz-Albite-Anorthite-Water. *Geochimica et Cosmochimica Acta*, 43, pp. 1131-1140.

[41] MARTODJOJO, S. (1984) *Evolusi Cekungan Bogor, Jawa Barat*. PhD Thesis, unpublished, Institut Teknologi, Bandung, Indonesia.

[42] REYES, A. G. (1990) Petrology of Philippine geothermal systems and the application of alteration mineralogy to their assessment. *Journal of Volcanology and Thermal Research,* 43(1-4), pp. 279–309.

[43] FULIGNATI, P. (2020) Clay minerals in hydrothermal systems. *Minerals*, 10(10), pp. 1–17, doi: 10.3390/min10100919,

[44] PERTAMINA (1995) Evaluasi Kelayakan Pengembangan Area Panasbumi Kamojang. *Laporan Internal PERTAMINA*

Divisi Panasbumi Direktorat Eksplorasi dan Produksi, Tim Pokja Kamojang, pp. 53, unpublish.
[45] PERTAMINA & BAFI-BATAN (1989) Laporan Akhir Inventarisasi Data Isotop dan Data Analisa Kimia Air Daerah P. Jawa dan Lapangan Kamojang. Hidrologi BAFI-BATAN, Kerjasama Dinas Geothermal Pertamina Pusat Jakarta dan BAFI-BATAN Jakarta, unpublished.
[46] ABIDIN Z. (2003) *Karakteristik Reservoar Panasbumi Untuk Manajemen Lapangan Uap Di Lapangan Kamojang Jawa Barat*. Doctoral Dissertation, Universitas Gajah Mada, unpublished.
[47] TAYLOR, H.P., JR. (1967) Oxygen Isotope Studies of Hydrothermal Mineral Deposits. In Barnes, H.L. (ed.), Geochemistry of Hydrothermal Ore Deposits. *Holt, Rinehart and Winston, Inc*., pp. 109-142.
[48] GARLICK, G.D. (1972) Oxygen Isotope Geochemistry. In FAIRBRIDGE, R.W. (Ed.). *The Encyclopedia of Geochemistry and Environmental Science*. Van Nostrand Reinhold Company, New York, pp. 864-874.
[49] FAURE, G. (1977) *Principles of Isotope Geology*. John Wiley and Sons, New York.
[50] HOEFS, J. (1980) *Stable Isotope Geochemistry*, Second Edition. Springer-Verlag, Berlin-Heidelberg, New York.
[51] HEDENQUIST, J.W. & RICHARDS, J. (1998) The Influence of Geochemical Techniques on The Development of Genetic Models for Porphyry Copper Deposits. In Richards and Larson (ed.). Techniques in Hydrothermal Ore Deposits Geology. *Economic Geology*, 10, pp. 235-256.
[52] CLAYTON, R. N. & STEINER, A. (1975) Oxygen isotope studies of the geothermal system at Wairakei, New Zealand. *Geochimica et Cosmochimica Acta*, 39(8), pp. 1179–1186, doi: 10.1016/0016-7037(75)90059-9

参考文:

[1] IBRAHIM, R. F., FAUZI, A., 和 SURYADARMA。(2005) 印度尼西亚地热能源活动的进展。土耳其安塔利亚世界地热大会论文集，第 1-7 页。https://www.geothermal-energy.org/pdf/IGAstandard/WGC/2005/0142.pdf
[2] WAHYUNINGSIH, R. (2005) 印度尼西亚地热开采的潜力和工作区域。研讨会，实地调查结果，印度尼西亚矿产资源清单理事会，万隆，（印度尼西亚语，附英文摘要）。http://psdg.bgl.esdm.go.id/kolokium/Makalah%20Umum/1.%20Makalah%20PB%20Potensi%20dan%20WKP%20Panas%20Bumi.pdf
[3] DEON, F., FÖRSTER, H. J., BREHME, M., WIEGAND, B. 等。(2019) 基于矿物学和热液蚀变的印度尼西亚地热勘探。I.O.P.会议系列：地球与环境科学，254(1)，土井：10.1088/1755-1315/254/1/012002。
[4] SURYANTINI, SETIJADJI, L.D., WAHYUNINGSIH, R., EHARA, S., 等。（2005）。印度尼西亚爪哇岛的地热田：描述、地质环境和初步选区勘探策略。第三届地球科学与技术国际研讨会论文集，九州大学，福冈，第 11-18 页。
[5] SETIJADJI, L.D. (2010) 分段火山弧及其与印度尼西亚爪哇岛地热场的关联。世界地热大会论文集，印度尼西亚巴厘岛，第 1-12 页。
[6] MARLIYANI, G. I., HELMI, H., ARROWSMITH, J.R., 和 CLARKE, A. (2020) 火山形态作为印度尼西亚爪哇火山弧应力方向的指标。火山学和地热研究杂志，400，文章 ID 106912，土井：10.1016/j.jvolgeores.2020.106912,
[7] UTAMI, P. (2000) 热液蚀变矿物学揭示的卡莫让地热储层（西爪哇）的特征。世界地热大会论文集，1921-1926 页。可在：http://web01.opencloud.dssdi.ugm.ac.id/wp-content/uploads/sites/395/2012/12/Characteristics-of-the-Kamojang-Geothermal-Reservoir-2000-Pri-Utami .pdf。
[8] KAMAH, MY, DWIKORIANTO, T., ZUHRO, AA, SUNARYO, D., 和 HASIBUAN, A. (2005) 基于微调器数据识

别的生产性进料区及其在卡莫让地热区储层潜力审查中的应用，印度尼西亚。世界地热大会论文集，土耳其安塔利亚，第 1-6 页。

[9] SUDARMAN S、BOEDIHARDI、M.、PUDYASTUTI、K.和 BARDAN。(1995) 卡莫让地热田 10 年运营经验。世界地热大会论文集，第 1773-1777 页。

[10] PENA-CASTELLNOU, S., INDAH MARLIYANI, G. 和 REICHERTER, K. (2019) 奥帕克断层系统的初步构造地貌学，爪哇（印度尼西亚）。埃古加, 21, 第 12307 页.

[11] SIEH, K., 和 NATAWIDJAJA D. (2000) 印度尼西亚苏门答腊断层的新构造。地球物理研究杂志，105(乙 12)，第 28295-28326 页。

[12] HALL, R., CLEMENTS, B., SMYTH, H. R., 和 COTTAM, M. A. (2007) 爪哇结构的新解释，印度尼西亚石油协会会议记录，第 1-23 页。可在以下网址获得：http://searg.rhul.ac.uk/pubs/hall_etal_2007 Java Structure_IPA.pdf。

[13] ANHAF, J. S. PATONAH, A., PERMANA, H., 和 ISMAWAN, I. (2018) 万丹巴亚复合区的结构和构造重建。地球科学、工程、环境和技术杂志，3(2)，第 77 页, 土井：10.24273/jgeet.2018.3.2.1554。

[14] HARYANTO, I., ILMI, N. N., HUTABARAT, J., ADHIPERDANA, B.G.，等。（2020）。古农克罗蒙，西爪哇，印度尼西亚的构造和地质结构。国际 GEOMATE 杂志，19(74)，第 185-193 页，土井：10.21660/2020.74.05449，

[15] PULUNGGONO 和 MARTODJOJO S. (1994) 古近纪-新近纪构造变化是爪哇中最重要的构造事件。中生代晚期到第四纪爪哇岛的地质和大地构造论文集，第 1-14 页。

[16] SOERIA-ATMADJA, R., MAURY, R. C, BELLON, H., PRINGGOPRAWIRO, H.，等。(1994) 爪哇第三纪岩浆带。东南亚和岩石学杂志，9，第 13-27 页，

[17] REJEKI, S., HADI, J., 和 SUHAYATI, I. (2005) 印度尼西亚西爪哇达拉贾特地热田储层详细特征的孔隙度研究。2005 年世界地热大会论文集，土耳其安塔利亚，https://www.geothermal-energy.org/pdf/IGAstandard/WGC/2005/0634.pdf

[18] ROBERT, D. (1988) 卡莫让地热田开发优化的地下研究。国家石油公司的 BEICIP/地理服务报告，第 47 页。

[19] ROBERT, D., RAHARSO R, 和 BASTAMAN S. (1983) 卡莫让地热田的勘探与开发。印度尼西亚石油协会会议记录，1，第 171 – 190 页。

[20] ROBERT, D. (1987) 卡瓦卡莫让地热西部的地质研究，PERTAMINA/BEICIP 报告，第 89 页。

[21] YUDIANTORO, D. F., SUPARKA, E., TAKASHIMA, I., ISHIYAMA, D., KAMAH, Y. (2012) 印度尼西亚西爪哇卡莫江地热田 KMJ-49 井蚀变岩石的蚀变和岩石地球化学。国际经济与环境地质学杂志，3(2)，第 21-32 页。

[22] YUDIANTORO, D. F., SUPARKA, E., YUWONO, S., TAKASHIMA, I.，等。(2013) 印度尼西亚卡莫让地热田的层间伊利石/蒙脱石。印度尼西亚地质杂志，地质局，4，第 177-183 页，http://ijog.bgl.esdm.go.id/index.php/IJOG/article/view/167/167

[23] UTAMI，P. R. I.；BROWNE, P. R. L. (1999) 印度尼西亚西爪哇岛卡莫让地热田的地下热液蚀变。第二十四次地热储层研讨会论文集，斯坦福大学，加利福尼亚州斯坦福。可在 https://citeseerx.ist.psu.edu/viewdoc/download?doi=10.1.1.545.7179&rep=rep1&type=pdf 获得

[24] KAMAH Y., TAVIP D. 和 AGUS A. Z. (2003) 克服印度尼西亚西爪哇卡莫让地热区东区块钻井作业中的地质问题。第六届印度尼西亚地热协会会议记录，第 175-184 页。

[25] PURBA, S. (1994) KMJ-48 和 53 卡莫让地热田西爪哇印度尼西亚井岩心和切割样品的热液蚀变，第 58 页，未发表。

[26] SUPARKA, K., YUDIANTORO, D. F., TAKASHIMA, I., HUTABARAT, J., 和 KAMAH, M. Y. (2013) 卡莫让地热田西爪

哇印度尼西亚的当前温度研究。第 2 届国际贸易局地热研讨会论文集 2013 万隆工艺学院，印度尼西亚万隆，第 1-8 页。可在：http://eprints.upnyk.ac.id/12123/

[27] YU, X., LIU, C., WANG, C., ZHAO, J.-X., 和 WANG, J. (2021) 江陵盆地上白垩统至下始新世地热水成因，华南：多同位素示踪剂和水-岩相互作用的约束。应用地球化学，124，文章 ID 104810，土井：10.1016/j.apgeochem.2020.104810

[28] BLASCO, M., AUQUE, L. F., GIMENO, M. J., ACERO, P., 和 ASTA, M. (2017) 碳酸盐-蒸发热系统化学特征中移动元素浓度的地球化学、地热测量和影响。蒂尔马斯地热系统（西班牙）的案例。化学地质学，466（5 月），第 696-709 页，土井：10.1016/j.chemgeo.2017.07.013，

[29] CRAIG, H. (1961) 大气水中的同位素变化。科学, 133(3465), 第 1702–1703 页, 土井: 10.1126/science.133.3465.1702

[30] CRAIG, H. (1966) 红海和索尔顿海地热盐水的同位素组成和起源。科学, 154(3756), 第 1544–1547 页，土井：10.1126/science.154.3756.1544,

[31] RICHARDSON, S. M. 和 MCSWEEN, H. Y. JR。(1989) 地球化学途径和过程。普伦蒂斯大厅，第 208-235 页。

[32] MICHELSEN, N. (2020) 干旱环境中选定水循环成分的同位素、化学和众包研究。可在：http://tuprints.ulb.tu-darmstadt.de/17657/

[33] FIELD, C. W. 和 FIFAREK, R. H. (1985) 浅热环境中的光稳定同位素系统学。在 BERGER，B.R. 和 BETHKE，下午（编辑）。浅热系统的地质学和地球化学，经济地质学评论，2，经济地质学家协会，第 99-128 页，

[34] CATHLES, L. M. (1983) 日本北陆盆地大量硫化物沉积的热液系统分析。在 OHMOTO, H. 和 SKINNER, B. J. (编辑。) 黑子和相关火山成因块状硫化物矿床：经济地质学，专着 5，第 439-487 页，

[35] TAYLOR，H. P. (1974) 氧和氢同位素研究在热液蚀变和成矿问题中的应用。经济地质学，69(6)，第 843-883 页，土井：10.2113/gsecongeo.69.6.843.

[36] TAYLOR, H.P., JR。（1979）热液矿床中的氧和氢同位素关系。在 BARNERS, H.L. (编。) 热液矿床地球化学，第二版，约翰威利父子，纽约，第 236-277 页.

[37] OHMOTO, H. 和 RYE, R. O. (1974) 黑子矿床流体包裹体的氢氧同位素组成。日本：经济地质学，69，第 947-953 页，

[38] GREEN, G. R., OHMOTO, H., DATE, J., 和 TAKAHASHI, T. (1983) 日本北六区深泽-小坂地区全岩氧同位素分布及其在矿产勘查中的潜在应用。经济地质学，75，第 395-411 页.

[39] SPOONER, E.T.C., BECKINSALE, R.D., ENGLAND, P.C., 和 SENIOR, A. (1977) 意大利乙. 利古里亚的蛇绿岩变质岩海底热液变质过程中的水合作用、18O 环境和氧化。地球化学与宇宙化学学报，41，第 857-871 页.

[40] MATSUHISA, Y., GOLDSMITH, J. R., 和 DAN CLAYTON, R. N. (1979) 石英-钠长石-钙长石-水系统中的氧同位素分馏。地球化学与宇宙化学学报，43，第 1131-1140 页.

[41] MARTODJOJO, S. (1984) 茂物盆地的演变，西爪哇。博士论文，未发表，印度尼西亚万隆理工学院。

[42] REYES, A. G. (1990) 菲律宾地热系统的岩石学和蚀变矿物学在其评估中的应用。43，第 279-309 页。

[43] FULIGNATI, P. (2020) 热液系统中的粘土矿物。矿物，10(10)，第 1-17 页，土井：10.3390/min10100919，

[44] PERTAMINA（1995）卡莫让地热区开发可行性评估。国家石油公司 内部报告

地热部勘探和生产局，卡莫让 工作组，第 53 页。

[45] PERTAMINA 和 BAFI-BATAN (1989) 爪哇岛和卡莫让油田水同位素数据清单和化学分析的最终报告。巴菲巴坦水文，中央国家石油公司地热服务和巴菲巴坦雅加达的合作，未发表.

[46] ABIDIN Z. (2003)。 西爪哇卡莫让油田蒸汽田管理的地热储层特征。论文博士，加也马达大学，未发表。

[47] TAYLOR, H.P., JR.（1967） 热液矿床的氧同位素研究。在 BARNES, H.L.（编辑）中，热液矿床的地球化学。 霍尔特，莱因哈特 和 温斯顿公司，第 109-142 页.

[48] GARLICK, G.D. (1972) 氧同位素地球化学。在费尔布里奇，R.W.（编辑） 地球化学与环境科学百科全书。 范诺斯特朗莱因霍尔德公司，纽约，第 864-874 页

[49] FAURE, G.（1977） 同位素地质学原理。 约翰威利父子，纽约.

[50] HOEFS, J. (1980) 稳定同位素地球化学，第二版，施普林格出版社，柏林-海德堡，纽约.

[51] HEDENQUIST, J.W. 和 RICHARDS, J.（1998）地球化学技术对斑岩铜矿成因模型发展的影响。在理查兹和拉尔森（编辑）。热液矿床地质技术。经济地质学，10，第 235-256 页.

[52] CLAYTON, R. N. 和 STEINER, A. (1975) 新西兰怀拉基地热系统的氧同位素研究。地球化学与宇宙化学学报，39(8)，第 1179-1186 页，土井：10.1016/0016-7037(75)90059-9，

ISOTOPE 18O OF ALTERATION ROCKS AT WELL C-1 KAMOJANG GEOTHERMAL FIELD, WEST JAVA, INDONESIA

ORIGINALITY REPORT

0%	0%	0%	0%
SIMILARITY INDEX	INTERNET SOURCES	PUBLICATIONS	STUDENT PAPERS

PRIMARY SOURCES

Exclude quotes	Off	Exclude matches	< 30%
Exclude bibliography	Off		